Macromolecules
ARTICLE

Macromolecules **2010**, *43*, 6877–6885 **6877**
DOI: 10.1021/ma1003826

Ejection of a Polymer Chain from a Nanopore: Theory and Computer Experiment

A. Milchev,*,†,‡ L. Klushin,§ A. Skvortsov,⊥ and K. Binder‡

†*Institute for Physical Chemistry, Bulgarian Academy of Science, 1113 Sofia, Bulgaria,* ‡*Institut für Physik, Johannes Gutenberg Universität Mainz, Staudinger Weg 7, 55099 Mainz, Germany,* §*Department of Physics, American University of Beirut, Beirut, Lebanon, and* ⊥*Chemical-Pharmaceutical Academy, Prof. Popova 14, 197022 St. Petersburg, Russia*

Received February 18, 2010; Revised Manuscript Received May 30, 2010

ABSTRACT: We consider the ejection dynamics of a flexible polymer chain out of confined environment. This situation arises in different physical contexts, including a flexible synthetic polymer partially confined in a nanopore and a viral genome partially ejected from its capsid. We describe the chain release from confinement both analytically and by means of dynamic Monte Carlo simulation. We find two distinct regimes of ejection dynamics depending on whether the chain is fully or partially confined. Partially confined chains are ejected from a pore of length L and diameter D after a typical time $\tau \propto L^2 D^{5/3}$, regardless of their contour length N. The process is driven by a *constant* force $f \approx 5k_BT/D$ and follows a "capillary" law. The force value is model-independent as long as the pore diameter exceeds the persistence length of the polymer chain and for pore walls that do not attract the segments of the polymer. In contrast, the ejection of fully confined chains is largely diffusive, the residence time being a nonmonotonic function of N. The drift-dominated ejection of long chains is characterized by narrow distribution of exit times whereas for diffusive-dominated ejection the exit times are described by a broad distribution. One finds good agreement with recent nanofluidic experiments with DNA.

I. Introduction

Properties of macromolecules in confinement are important for many areas of science and technology. Examples include the translocation of polymers through nanopores[1−3] partitioning of polymers from solutions into nanopores[4,5] packaging of DNA inside of virus capsids[6−11] or nanofluidic devices.[12,13] Despite intensive research during the past decades,[15−25] the quantitative and sometimes even the qualitative picture of polymer-in-pore behavior remain elusive. Recent experiments[5,12] have provided a series of fascinating results on the kinetics of polymer release from confinement. For relatively short macromolecules initially confined in tubes the residence time, i.e., the time required for the polymer to completely vacate the tube, shows a nonmonotonic behavior with respect to the chain molecular mass, first increasing and then decreasing again.[5] Above some threshold value of the polymer molecular mass the residence time becomes nearly insensitive to further polymer mass increase.[5] Traditional theoretical description of a homopolymer chain in a cylindrical tube includes three competing length scales that define the system: the chain contour length Na, the persistence length l_P of a free chain, and the confinement length D (the tube diameter). The tube itself is considered to be infinitely long. The existing scaling theory describes very well the equilibrium and dynamic aspects of chain behavior as confirmed by simulations.[26] The chain ejection experiments, however, contain explicitly yet another length paremeter, namely, the tube length L. Depending on the polymer molecular mass, the initial chain conformation could be fully confined for relatively short chains or only partially confined with a fraction of the chain comprising a tail outside the pore. The ejection kinetics turns out to be qualitatively different in these two cases. One possible theoretical approach to understand the ejection kinetics has been already briefly sketched,[23] but no detailed study has yet been made.

Inhomogeneous flowerlike conformation with partially confined stem and a free tail appears naturally in the process of expulsion of a single chain out of dense polymer brushes in a good solvent.[27] The same conformation has also been observed in experiments where an external electric field was used to drive an assembly of DNA molecules into tubes.[12] Upon switching the field off, partiually confined molecules were seen to recoil back into the free region. Expulsion kinetics involving partially confined macromolecules has important implications for biological processes *in vivo*. These include ejection of phage genome from a capsid[11] or ejection of a polymer from a protein channel in a lipid membrane.[5]

In this paper we present computer modeling and analytical theory describing the ejection kinetics. We predict the residence time of a polymer, confined in a narrow pore, in dependence of the contour and persistence lengths of the chain, the tube diameter, and the initial position of the chain regarding the open end of the tube. We demonstrate that ejection of fully confined chains is dominated by simple diffusion along the tube while the motion of *partially* confined chains is close to deterministic drift subject to *constant* driving force. Thus, the dominant ejection mechanisms are qualitatively different in these two cases.

Recent developmens in micro- and nanofabrication by chip lithography provide a powerful tool for producing channels of precise geometry with characteristic dimensions on the scale of tens to hundreds of nanometers. Experiments with DNA driven by pulsed electric field into nanofluidic devices open up venues for developing new separation methods for enormously large DNA molecules with unprecedented resolution.[14,28] Our paper can be considered as a basis for the theory of such separation.

*To whom correspondence should be addressed.

Published on Web 07/28/2010

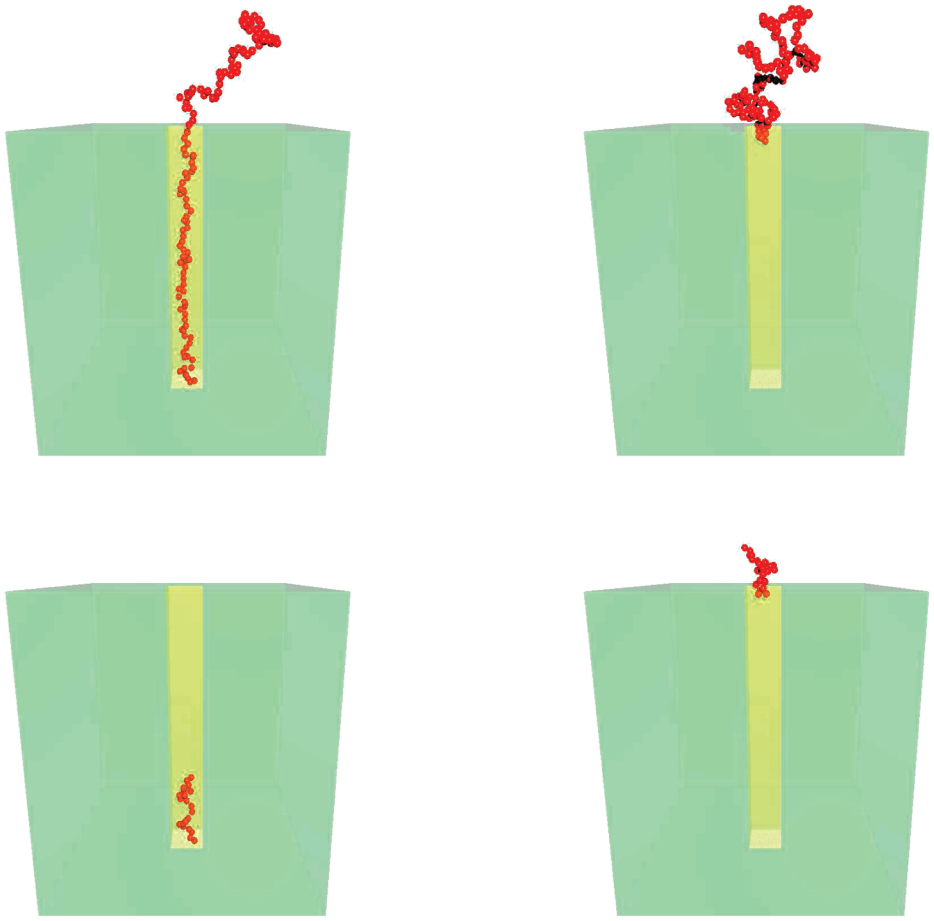

Figure 1. Snapshots of an initial (left) and final (right) polymer chain conformation, placed in a rectangular nanopore of side $D = 2$ within a semitransparent impenetrable matrix. The pore exit is at height $L = 30$. The chain length is $N = 128$ (above) and $N = 24$ (below).

The paper is organized as follows: after this Introduction, in section II we give a brief description of the model and Monte Carlo method of simulation. In section III we present the results of scaling theories for long chains in infinite tubes. In section IV we present theory and simulation data concerning the ejection time of flexible chain fully and partially confined in a nanotube in dependence on chain's length and pore width. We demonstrate in section IV.A the governing "capillary" law of chain motion during ejection and in section IV.C present the theory results for the distribution of ejection times and compare predictions with simulation data. In section V we discuss briefly the impact of persistence length on the force of ejection and the way hydrodynamic interactions affect the kinetics, and in section VI we end this scientific report by emphasizing the main conclusions which follow from our investigation.

II. Model and Method

Our system is shown in Figure 1. Nanopore was modeled as a channel of square cross section $D \times D$ with impenetrable walls which is sealed at depth L and has one open end. The polymer chain is placed in this pore with end monomer of the chain initially anchored in the bottom of the pore. Short chains are fully confined in pore. Sufficiently long chains have a tail outside the pore. Thus, the polymer segments are confined between structureless and impenetrable walls. The pore diameter D has been varied in the range $D = 2-6$ and the pore length in the range $L = 16-35$.

We have used a coarse-grained off-lattice bead spring model[29] to describe the polymer chains. The effective bonded interaction is described by the FENE (finitely extensible nonlinear elastic) potential:

$$U_{\mathrm{FENE}} = -K(1-l_0)^2 \ln\left[1-\left(\frac{l-l_0}{l_{\max}-l_0}\right)^2\right] \qquad (2.1)$$

with $K = 20$, $l_{\max} = 1$, $l_0 = 0.7$, and $l_{\min} = 0.4$

The nonbonded (excluded volume) interactions are described by the Morse potential

$$\frac{U_{\mathrm{M}}(r)}{\epsilon_{\mathrm{M}}} = \exp[-2\alpha(r-r_{\min})] - 2\exp[-\alpha(r-r_{\min})] \qquad (2.2)$$

with $\alpha = 24$, $r_{\min} = 0.8$, and $\epsilon_{\mathrm{M}}/k_{\mathrm{B}}T = 1$. With this choice of units the mean distance between beads in the simulations is found to be $a = 0.766$. For this model the Θ-temperature is at $k_{\mathrm{B}}T/\epsilon_{\mathrm{M}} = 0.62$[29] so the chain is in the good-solvent regime.

One advantage of this model is that in bulk solutions it approaches the scaling region rather rapidly; already relatively short chains exhibit power laws with effective exponents close to the asymptotic behavior. In the present work we use chain length N up to $N = 256$, and our observations (see Figure 2a) indeed indicate a very good agreement with the expected scaling behavior of a polymer in a tube.

The size of the container box was $128 \times 128 \times 128$. The standard Metropolis algorithm was employed to govern the moves with self-avoidance automatically incorporated in the potentials. In each Monte Carlo update, a monomer was chosen at random and a random displacement attempted with Δx, Δy, Δz chosen uniformly from the interval $-0.5 \le \Delta x, \Delta y, \Delta z \le 0.5$. The transition probability for the attempted move was calculated

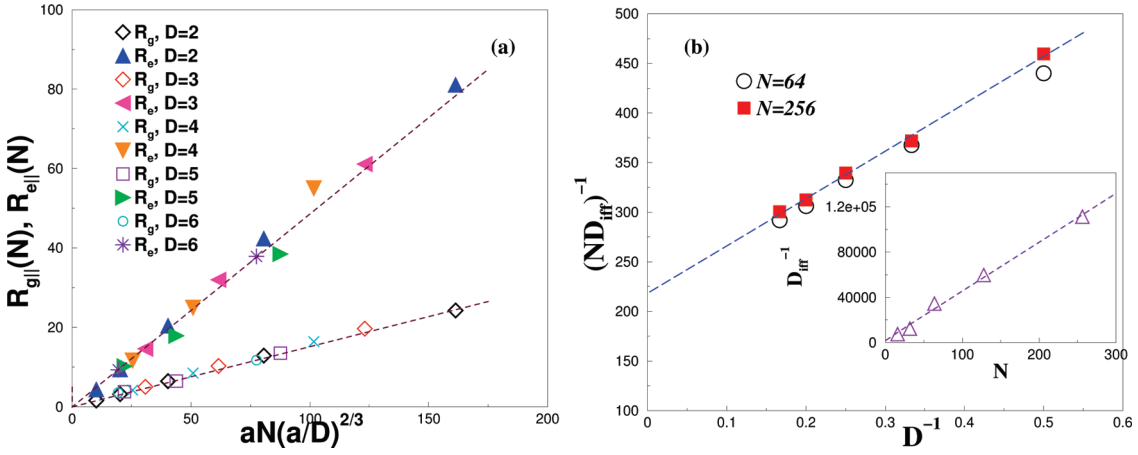

Figure 2. (a) Variation of the end-to-end distance R_e and gyration radius R_g of a flexible self-avoiding polymer chain against scaling variable $ND^{-2/3}$ for different chain length N and different tube diameter D. (b) Effective friction coefficient $\zeta = (ND)^{-1}$ (per monomer) against inverse tube diameter D^{-1} for two different chain lengths $N = 64, 256$. In the inset we show the variation of the total friction coefficient of the chain D^{-1} with the number of monomers N.

from the change ΔU of the potential energies before and after the move as $W = \exp(-\Delta U/k_BT)$. As for a standard Metropolis algorithm, the attempted move was accepted if W exceeds a random number uniformly distributed in the interval [0,1). A Monte Carlo Step (MCS) is elapsed when all N monomers of the chain are selected at random and given the chance to perform an elementary move. The chain length was varied in the range $N = 4-256$. Except for the shortest chains, the pore diameter is smaller than radius of gyration R_g of a chain in free volume. In order to study the mechanism of chain ejection from the pore, we keep initially the last monomer fixed at the sealed bottom of the pore $z = 0$ while the polymer chain of a particular length N is equilibrated for a period of about 65 536 MCS. Then the link of the last monomer with the bottom of the pore is removed, and the chain is released to diffuse along the tube. While the chain escapes from confinement, we record the temporal position of the last monomer in the tube as well as the pulling force exerted on it by the rest of the segments. The ejection time τ is measured, once this last monomer passes the opening at $z = L$ and leaves the pore. After the chain is ejected from the pore, it is replaced by a new one in the starting position, equilibrated while anchored, and then released for the subsequent run again. Our averages are then taken typically on 500−5000 runs. We find that the ejection times, observed in the simulation, range between 10^3 and 10^7 MCS, depending on N, D, and L.

III. Chain in Infinitely Long Nanopore

We start with the analysis of the typical chain conformation in an infinitely long tube. In this case the entire chain may be thought of as a linear sequence of blobs. Each blob of size $D \propto ag^{\nu}$ contains g segments, where a is the segment size, and the value of the Flory exponent ν is approximately 3/5. The number of blobs $n_b = N/g$ scales as

$$n_b = N\left(\frac{a}{D}\right)^{5/3} \tag{3.1}$$

The average end-to-end distance R_e of a fully confined chain is the number of blobs n_b times the blob size D; therefore

$$R_e = A_e Na\left(\frac{a}{D}\right)^{2/3} \tag{3.2}$$

where A_e is a model-dependent prefactor of order unity. This relation was confirmed by simulations[21,30] and also by experiments.[31]

The free energy of a long flexible chain in an infinite tube is given by

$$\frac{F_{conf}}{k_BT} = A_F n_b = A_F N\left(\frac{a}{D}\right)^{5/3} \tag{3.3}$$

where A_F is another nonuniversal prefactor. Burkhardt and Guim[32] produced a rigorous theoretical proof that the relation between F_{conf} and R_e in the scaling regime $Na \gg D \gg a$ is much more universal:

$$\frac{F_{conf}}{R_e} = B\frac{k_BT}{D} \tag{3.4}$$

The numerical coefficient B is *model-independent*; i.e., it has the same value for all polymer chains in good solvents. The parameters of the system that do affect the value of B include the spatial dimension d, the universality class of the monomer−tube interaction (repulsion, adsorption, or critical adsorption point), the universality class of the monomer−monomer interaction (good, poor, or θ-solvent), and the tube geometry (circular vs rectangular cross section). Calculations[32] based on field-theoretical methods gave $B = 2.12 \pm 0.01$ for 2d geometry (strip) and hard-wall boundaries. This is remarkably close to the results obtained by Monte Carlo simulations for self-avoiding walks on a square lattice confined to infinite strips, $B = 2.125$.[33] MC simulations of fully confined self-avoiding chains on a simple cubic lattice in 3d tubes of circular cross sections produced the values $A_e = 0.92 \pm 0.03$ and $A_F = 5.33 \pm 0.05$.[34] These values are reached asymptotically for long enough chains with $n_b \gg 1$, and their ratio is $B = 5.79$. According to arguments of Burkhardt and Guim,[32] the relationship

$$\frac{F}{R_e} = 5.79\frac{k_BT}{D} \tag{3.5}$$

is universal and applies to all chains in tubes with circular cross section in the scaling regime. No direct data are available for tubes of square cross section, and henceforward we will use the value $B = 5.79$ as an estimate for our case.

It is convenient to introduce the strain parameter $\lambda = R_e/Na$ describing the average elongation of the chain in a pore with respect to its contour length. In the scaling regime $\lambda = A_e(a/D)^{2/3}$.

If hydrodynamic interactions are ignored, the dynamics of a chain in a tube is well described by the Rouse model. The characteristic time τ_{dif} for diffusion of a polymer along a narrow

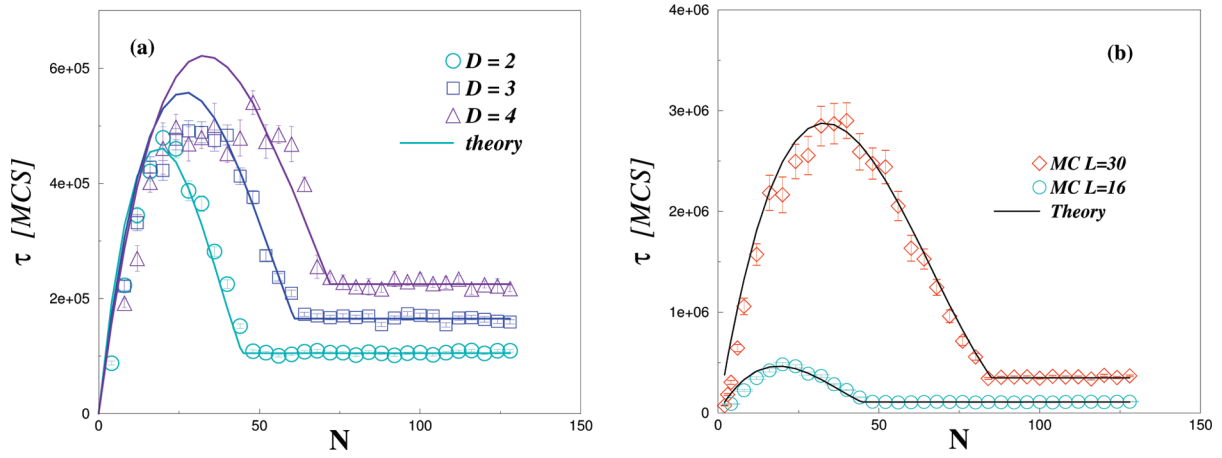

Figure 3. (a) Average ejection time τ against polymer length N for chains in a pore with length $L = 16$ and different pore diameters $D = 2, 3, 4$. The error bars result from 400 ejection attempts. (b) The same for pores of length $L = 16$ and $L = 30$ and diameter $D = 2$. The full lines are given by eqs 4.8 and 4.12. Evidently, for chains beyond certain critical length N^* the ejection time τ is independent of N!

tube $D \ll R_g$ on a distance of the order of its own size is found from the relation

$$\tau_{dif} = \frac{R_e^2}{2\mathscr{D}} \tag{3.6}$$

whereas the diffusion coefficient $\mathscr{D}$ is

$$\mathscr{D} = \frac{k_B T}{N\zeta} \tag{3.7}$$

where ζ is the friction coefficient per monomer. It follows from the above equations that the characteristic time of a chain, diffusing in a tube, scales as

$$\tau_{dif} \propto N^3 D^{-4/3} \tag{3.8}$$

in accordance with computer simulations.[19]

The variation of the average end-to-end distance R_e and the average gyration radius R_g of self-avoiding off-lattice chains vs the scaling variable $ND^{-2/3}$ for several chain lengths and tube diameters is displayed in Figure 2. Although the tube diameters include the values down to $D/a = 2.6$, there are no pronounced deviations from the scaling prediction, eq 3.2. The slopes provide estimates for the two numerical coefficients $A_e = 0.746$ and similarly for the gyration radius $A_g = 0.234$. Note that our monomer size $a \approx 0.766$ and not unity. The diffusion coefficient $\mathscr{D} \propto N^{-1}$ (see the inset of Figure 2b), which is characteristic of free-draining diffusive motion. One can define the effective friction coefficient per monomer as $\zeta = (N\mathscr{D})^{-1}$. The dependence of the friction coefficient ζ on the tube diameter is shown in Figure 2b, and is well approximated by a simple expression

$$\zeta = \zeta_{vol} + \zeta_{surf}\frac{a}{D} \tag{3.9}$$

where $\zeta_{vol} \approx 218.3$ is the friction coefficient in the absence of the tube and $\zeta_{surf} \approx 623$ can be interpreted as an extra friction due to the walls.

IV. Ejection Kinetics for Short and Long Chains

One of the main results from the Monte Carlo simulation is displayed in Figure 3a where we show the average time of ejection in dependence of the chain length N in pores with different diameters $D = 2, 3, 4$ at the same length $L = 16$. Figure 3b shows the effect of pore length for $L = 16, 30$ at the same diameter $D = 2$.

It is clear that there are two regimes. For short chains the ejection time depends on N nonmonotonically whereas for long chains it is practically independent of N. A crossover between these regimes occurs at a critical chain length N defined by the condition $R_e(N^*) = L$, which gives

$$N^* = \frac{L}{a\lambda} \tag{4.1}$$

The short chains with $N < N^*$ are initially fully confined inside the tube while the long chains with $N > N^*$ have a tail outside the tube opening. In order to explain this unusual behavior, we consider below the two regimes separately.

A. Long Chains with Tail ($N > N^*$). We start with the ejection regime of long chains $N > N^*$ having a tail outside the tube. It was shown in[23] that the tail outside a tube opening creates a pulling force of entropic origin acting on the confined part of the chain which is *independent* of the tail size (as long as it exceeds the blob size). One may understand the existence of such force by considering the free energy F of a chain partially confined in a tube with the inner chain end being at distance x from the tube opening (see ref 23). The total free energy F is due to the confined part of the chain and is proportional to its lateral size. We use eq 3.5 to relate F to the end-to-end distance of the confined part, x:

$$F = B\frac{k_B T}{D}x \tag{4.2}$$

The slope of the free energy as a function of x has the meaning of an average force acting on the inner end-monomer:

$$f = B\frac{k_B T}{D} \tag{4.3}$$

with $B = 5.79$. A more comprehensive analysis, given in ref 23, shows that the numerical value of B is slightly lowered when the elastic response of the chain is accounted for. However, the effect is rather small, and in this paper we are not concerned with this difference. When all monomeric units are confined, the free energy does not depend on the end position x and the pulling force is equal to zero.

Langevin dynamics simulations have been performed for an ideal flexible chain, partially confined in an open cylindrical pore whose diameter was slightly larger than the monomer size.[11] This work demonstrates that the force is

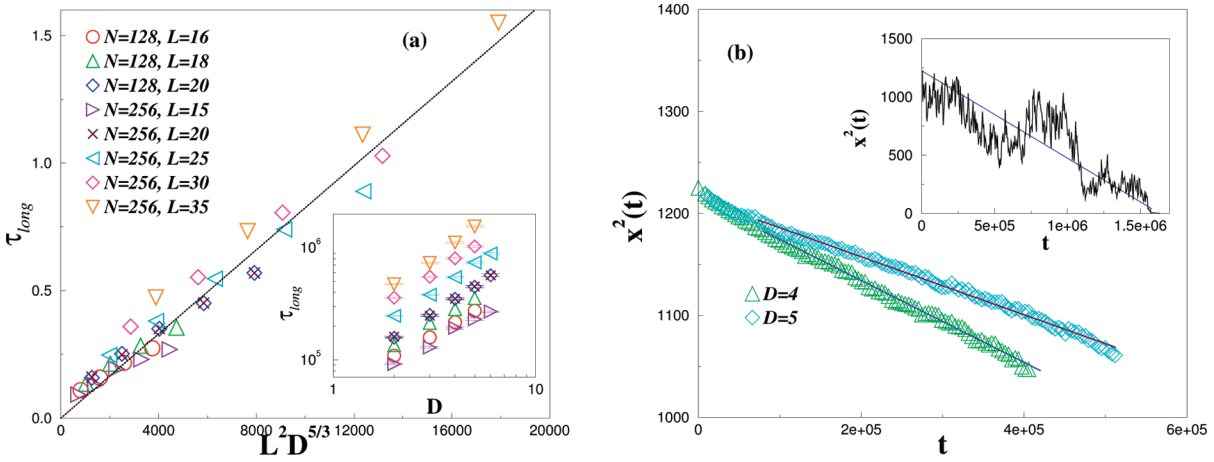

Figure 4. (a) Scaling plot of the ejection time τ_{long} with variable $L^2D^{5/3}$ for chain sizes $N = 128$, 256 and different pore lengths L. The inset shows the row data for τ_{long} on a logarithmic scale. (b) Squared distance $x^2(t)$ of the last monomer from the pore exit against elapsed time from the onset of the ejection process. Here $N = 256$ and $L = 35$. Solid lines denote the theoretical prediction, eq 4.7. A single trajectory for $D = 5$ is shown in the inset.

essentially independent of the tail length and of the length of the confined part of chain and decreases with growing D.

Ejection of the chain in the presence of a constant force can be described by choosing the end-monomer position inside the tube, x, as a dynamic variable. The distance is counted from the tube opening (see Figure 1). Balancing the pulling force, f, and the total friction (drag force), acting on all monomers inside the tube, yields the equation of motion

$$\zeta n(t)\frac{dx}{dt} = f \tag{4.4}$$

where ζ is the friction coefficient per monomer, n is the number of monomers still inside the tube, and the chain is assumed to be free-draining. The time-dependent variables x and n are related to each other by

$$x(t) = n(t)\lambda a \tag{4.5}$$

For simplicity, we assume that the dynamic strain parameter, λ, is time-independent and coincides with that in the static situation $\lambda \propto D^{-2/3}$. Then the equation of motion can be integrated to give

$$x^2(t) = x^2(0) - \frac{2f\lambda a}{\zeta}t \tag{4.6}$$

With $x(0) = L$, eq 4.6 yields

$$x^2(t) = L^2\left(1 - \frac{t}{\tau_{long}}\right) \tag{4.7}$$

whereby the condition $x(\tau) = 0$ yields the ejection time of the long chains (with a free tail)

$$\tau_{long} = \frac{\zeta}{2f\lambda a}L^2 \tag{4.8}$$

Equation 4.6 can be recognized as the law of time-reversed capillary flow. This law appears naturally for systems driven by a constant force provided the total friction changes proportionally to the front displacement. In our case this friction is related to those monomers which are inside the tube.

Hence, according to eq 4.8, the ejection time of chains with $N > N^*$ scales as

$$\tau_{long} \propto L^2D^{5/3} \propto N^{*2}D^{1/3} \tag{4.9}$$

It does not depend on the size of the free tail as is clearly demonstrated by Figure 3. In fact, the length independence of the ejection time for long polymers is essentially replaced by the quadratic dependence on the pore length L (cf. eq 4.8). It is therefore remarkable that polymer ejection is governed only by the pore length L and the tube diameter D.

The scaling plot of the ejection times τ_{long} with variable $L^2D^{5/3}$ is presented in Figure 4 for two chain sizes $N = 128$, 256 and different tube lengths L. The inset shows the raw data for τ_{long} vs pore diameter D on a logarithmic scale.

The master curve in Figure 4a confirms the prediction eq 4.9. The data in the inset fall on straight lines with a slope ≈1.25−1.32. Note that for a given pore length $L = 20$ the times of ejection τ_{long} *coincide* regardless of the polymer size $N = 128$ or $N = 256$, thus validating one of the main theoretical predictions of section IV.

The squared distance $x^2(t)$ between the last monomer and the pore exit against elapsed time from the onset of the ejection process is presented in Figure 4b for $N = 256$, $L = 35$, and tube diameters $D = 4$, 5. The curves are well approximated by straight lines as suggested by eq 4.6 with the slope proportional to the ratio f/ζ.

Similar curves were obtained experimentally[12] for the $T2$ phage DNA molecules with contour length 51 μm. DNA monodisperse molecules were pushed into tubes with $D = 35$ nm by pulsed electric field. The recoil of the molecules into free region was recorded by fluorescence video microscopy, and the end point position as a function of time was fitted by an equation very similar to eq 4.6.

In our simulations, we measure directly the fluctuating force acting on the last monomer of the confined chain both before and after the chain is released from the anchoring point (see Figure 5). Each fluctuating curve results from averaging over 500 independent runs. Smooth curves are obtained by additional averaging over a short time window. Each curve starts with a plateau level that depends only on the tube diameter D. Individual trajectories would show a sharp drop in the time-averaged force at the moment the last few monomers (comprising a blob) leave the tube. Owing to a distribution of the first passage times, steplike individual trajectories average out to smooth curves decreasing to zero with time. The force

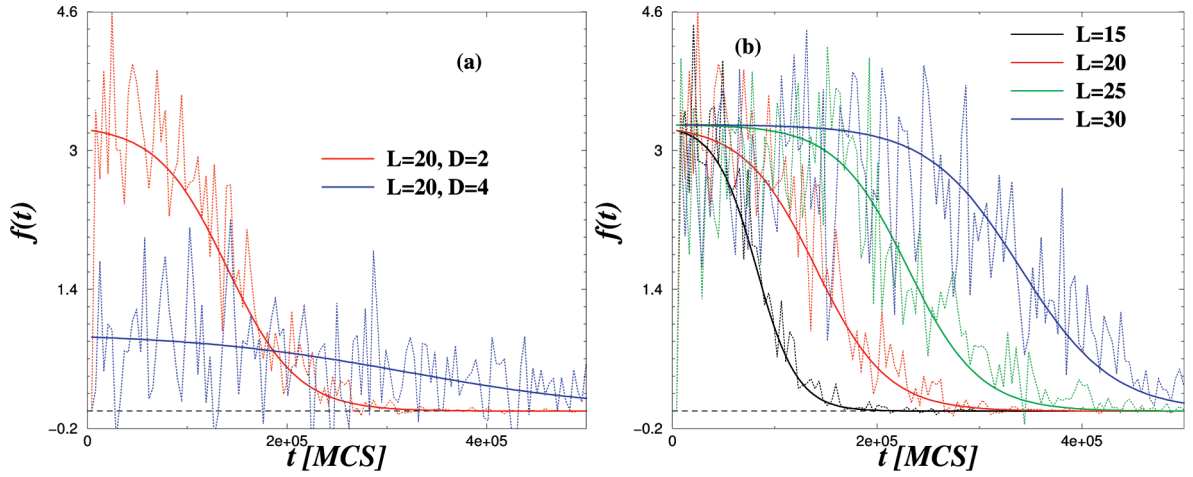

Figure 5. (a) Force, f, exerted on the last (innermost) monomer of a chain with $N = 256$ against time for $L = 20$ and two different pore diameters D. (b) The same for $D = 2$ and several pore lengths $L = 15, 20, 25, 30$. All the stochastic curves are averages over 500 runs. The solid lines correspond to additional averaging over a short time window (10 MCS). A dashed horizontal line indicates $f = 0$.

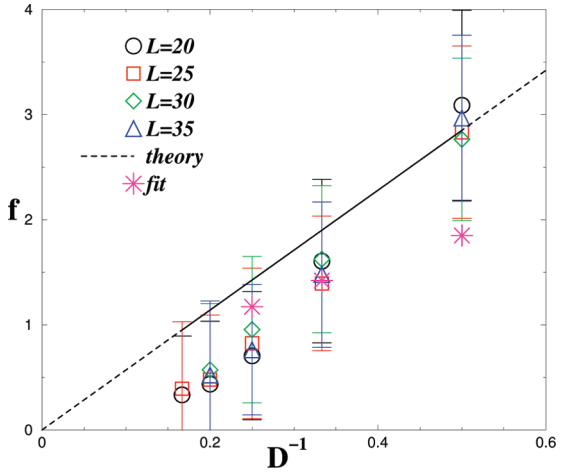

Figure 6. Time-averaged force f on the last monomer against inverse tube diameter. Error bars indicate the variance over time of 500 measurements. The straight line is drawn according to eq 4.3. Also shown are indirect estimates of the mean force obtained by fitting the curves of Figure 3 (fit) as explained in section IV.B.

plateaus correspond to the situation when the chain is still partially residing in the tube in all the trial runs. The plateau values of force f are presented in Figure 6 against the inverse tube diameter. Error bars indicate the variance of the stochastic curves averaged over 500 runs. The straight line in Figure 6 is drawn according to eq 4.3. We also show indirect estimates of the mean force obtained from fitting the whole set of simulation curves $\tau(N)$ of Figure 3 with theoretical eqs 4.8 and 4.12. One may readily see that the scattering of points is quite significant and the prediction, $f \propto D^{-1}$ (see eq 4.3), is reproduced in the simulation with some deviations. Most of the data points lie below the theoretical straight line, suggesting a somewhat smaller value of the coefficient $B \approx 5$.

B. Short Chains with $N < N^*$. The ejection process of the short chains with $N < N^*$ which are initially fully confined in the tube occurs in two stages. First, the chain must approach the tube opening in order to be able to form a tail. At this stage there is no net force acting on the chain and the motion is described by simple diffusion with a reflecting boundary condition at the closed end of the tube. Evaluation of the duration of this diffusive stage is straightforward. In order to reach the opening, the chain must cover a distance $L - R_e$, moving with diffusion coefficient $\mathscr{D}$. The mean first passage time for such a diffusive process is given by[38]

$$\tau_1 = \frac{(L - R_e)^2}{2\mathscr{D}} \tag{4.10}$$

Once a tail is formed, the pure diffusion is replaced by a motion due to the constant pulling force. In this second stage the diffusive contribution is expected to be less important, and the motion should become nearly deterministic. Equation 4.6 still applies, but the initial value $x(0)$ is now related to the end-to-end distance, $x(0) = R_e = \lambda N a$:

$$\tau_2 = \frac{a\lambda\zeta}{2f}N^2 \tag{4.11}$$

Adding together the two contributions gives a simple (albeit not rigorous) estimate for the full ejection time of the short chains:

$$\tau_{\text{short}} = \frac{N\zeta}{2k_B T}(L - Na\lambda)^2 + \frac{a\lambda\zeta}{2f}N^2 \tag{4.12}$$

For chains that are not too close to the critical length N, the diffusive stage provides the dominant contribution to the total time of ejection τ. This corresponds to the following condition:

$$N^* - N \gg \sqrt{\frac{Nk_B T}{fa\lambda}} \tag{4.13}$$

The maximum residence time is achieved for short chains with $N = N^*/3$, yielding

$$\tau_{\max} = \left(\frac{2\zeta}{27\lambda a}\right)L^3 \tag{4.14}$$

The scaling theory predicts that the ratio of $\tau_{\max}$ and the ejection time of long chains, τ_{long}, depends only on L/D:

$$\frac{\tau_{\max}}{\tau_{\text{long}}} = \left(\frac{4B}{27}\right)\frac{L}{D} \tag{4.15}$$

The theoretical predictions (4.10) and (4.12) were used to describe the $\tau(N)$ curves of Figure 3, produced by simulations. The values of the monomer friction coefficient in tubes of various diameters were taken from the data for diffusion of the $N = 64$ chain in infinite pores. These data are representative of the chain lengths in the vicinity of N^* in

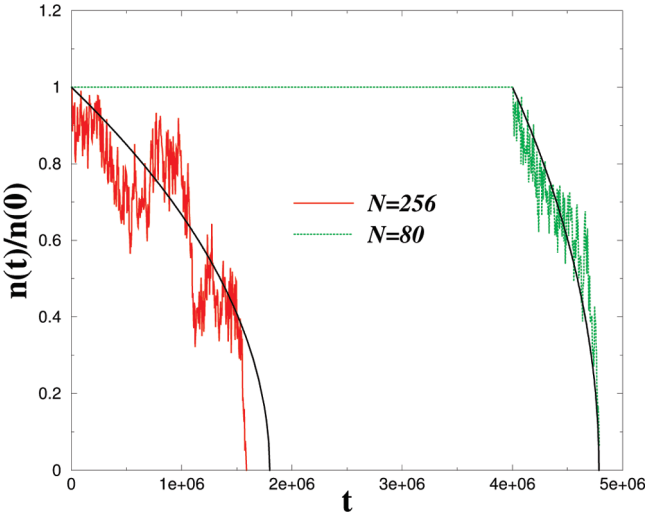

Figure 7. Number of monomers $n(t)$ inside the tube (normalized by its value at $t = 0$) against elapsed time t from the onset of ejection for a long chain $N > N^*$ (full line) and a short chain $N < N^*$ (dashed line) in a pore with $L = 35$ and $D = 5$ where $N^* = 117$. The diffusive regime of the fully confined short chain whereby $n(t) = n(0)$ is indicated by a horizontal line. Solid black lines indicate the theoretically predicted "capillary" law, eq 4.16.

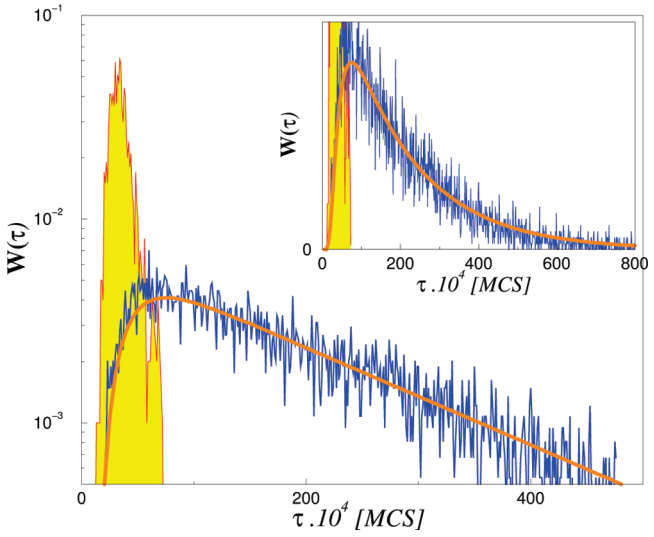

Figure 8. (a) Probability distribution of the ejection time (first passage distribution) $W(\tau)$ for polymer chains in a narrow pore with diameter $D = 2$ and length $L = 30$ in semilog coordinates. A short chain with $N = 16$ is originally confined deep in the pore (blue line), whereas for a long chain with $N = 128$ (filled red curve) the tail is always outside the pore. Full line denotes a fit with the analytic function, eq 4.17. The inset shows the same in normal coordinates.

most pores. The nonmonotonic curves $\tau(N)$ of the short chain regime contain the strain parameter λ. The values of $\lambda(D)$ were also taken from the data on chains in infinite tubes. It turned out that in order to achieve the best fit for the relatively short tube of length $L = 16$ the values of λ had to be slightly corrected by a factor of 0.9 while for chains in the longer tube with $L = 30$ the correction factor was 0.96. No other adjustable parameters were used to produce the nonmonotonic theoretical curves in Figure 3.

One can notice that the theoretical maxima are quite pronounced while the simulation data points appear to give "flattened" maxima. This is due to the fact that some of the runs with $L = 16$ were not long enough to explore accurately the late-time tail of the residence time distribution $W(\tau)$, thus providing an underestimate of the mean ejection time (see the next subsection for a more detailed discussion).

The flat portions of the $\tau(N)$ curves, representing the force-driven ejection, were employed to produce the indirect estimate of the force according to eq 4.8 (using the corrected values of $\lambda(D)$ obtained before). The resulting values of f appear in Figure 6 as "fit" estimates.

The number of monomers inside the tube as a function of time, $n(t)$, can be deduced from eq 4.7. After normalizing $n(t)$ by its initial value, the result may be presented in a compact form

$$\frac{n(t)}{n(0)} = \sqrt{1 - \frac{t}{\tau_{\text{long}}}} \tag{4.16}$$

It is clear that the above equation represents the capillary $\sqrt{t}$ law where the time is counted backward from the moment of exit. A similar expression would describe the second stage of the short chain ejection, if τ_{long} is replaced by τ_2 (see eq 4.11). The $n(t)$ dependence can be directly measured by fluorescence video microscopy.[12,14] For illustrative purposes we show two representative samples of $n(t)/n(0)$ curves obtained from individual Monte Carlo runs for $L = 35$, $D = 5$ and two chain lengths $N = 256$, $N = 80$ (Figure 7). The critical polymer length for this pore is $N^* = 117$. For the long chain $N = 256$ the stochastic trajectory follows the theoretical prediction rather closely, although the noise is also quite prominent. The diffusive regime of the short chain is represented by a horizontal line since all monomers remain inside the pore, $n(t) = n(0) = N$. Once the tail is formed, time-reversed capillary law sets in. For a short chain individual curves from different runs may differ dramatically by the moment the tail is first formed. This reflects the fact that diffusive first passage times are characterized by a broad distribution.

C. Residence Time Distribution. Residence (or ejection) time distribution, $W(\tau)$, is shown in Figure 8 for two polymers with lengths $N = 16$ and $N = 128$ in a pore with $D = 2$ and $L = 30$. The critical chain length for this pore is known to be $N^* \approx 48$. The theoretical description of the residence time distribution for long chains is mathematically involved and therefore falls outside the scope of the present paper. It is clear from the graph that this distribution for a long chain is rather narrow, consistent with the fact the ejection process is force-driven. For short chains the residence time is dominated by simple force-free diffusion. From the theoretical point of view, the relevant Fokker−Planck equation describing the residence time distribution can be mapped onto a simple diffusion problem with one reflecting and one adsorbing boundary condition.[39] The exact solution is given by

$$W(\tau) = \frac{2\pi\mathscr{D}}{l^2}\sum_{k=0}^{\infty}(-1)^k\left(k+\frac{1}{2}\right)\exp\left\{-\left[\frac{\pi\left(k+\frac{1}{2}\right)}{l}\right]^2\mathscr{D}\tau\right\} \tag{4.17}$$

whereby at short and long times the right-hand side of eq 4.17 yields the following asymptotics

$$W(\tau) = \begin{cases} \dfrac{1}{\sqrt{\pi}(\mathscr{D}\tau)^{3/2}}\exp\left(-\dfrac{l^2}{4\mathscr{D}\tau}\right), & \text{for } \tau \to 0 \\ \dfrac{\pi\mathscr{D}}{l^2}\exp\left(-\dfrac{\pi^2}{4l^2}\mathscr{D}\tau\right), & \text{for } \tau \gg 1 \end{cases} \tag{4.18}$$

where $l = L - \lambda aN$ is the diffusion distance. The true mean first passage time for diffusion $\langle\tau\rangle$ coincides exactly with the simple estimate $\langle\tau\rangle = l^2/2\mathscr{D}$.

For the short chain $N = 16$ one observes a perfect agreement (with no adjustable parameters) of the sampled PDF with the corresponding solution 4.17 if we use a diffusion coefficient $\mathscr{D} = 2.0 \times 10^{-4}$, which is very close (within error bars) to the value of $\mathscr{D} = 2.5 \times 10^{-4}$ found earlier (cf. Figure 2). It is also evident from Figure 8 that the long chain with a tail in the open ($N = 128$) takes much shorter time to leave the pore than the short chain, $\tau(N = 16)/\tau(N = 128) \approx 8$, even though in the latter case originally nearly 3 times more chain segments are confined in the pore.

V. Discussion

Biological polymers are generally charged and stiff on length scales much larger than their monomer size. In the native state the DNA is a polyelectrolyte; however, with the buffer concentration used in experiments,[12] the Debye screening length was about 0.7 nm. The presistance length of DNA is estimated as 50 nm. In the experiments reported in ref 12 the contour length of the T2 phage DNA was nearly 51 μm, and the number of Kuhn segments was close to 10^3. The strain parameter λ for DNA in a tube of diameter $D \simeq 110$ nm was estimated visually as 0.35.

In our Monte Carlo simulations we use a model of a fully flexible chain with persistence length of the order of monomers size, a. For real flexible polymers $a \approx 1$ nm. The strain parameter was about $\lambda = 0.15$ in wider tubes and increased up to $\lambda = 0.32$ in the narrowest tube of diameter $D = 2$. At this relative elongation the blob picture is essentially correct. It can be applied equally well to semiflexible chains as long as the tube diameter is large compared to the persistence length $D \gg l_P$.

We would like to emphasize that the opposite regime of very strong confinement of semiflexible chains specified by the condition $D < l_P/2$ is also well understood from the theoretical point of view.[35] In this regime the chain can be approximated as a weakly curved rod of finite flexibility with the mean end-to-end distance

$$R_e = Na\left[1 - A_1\left(\frac{2D}{l_P}\right)^{2/3}\right] \tag{5.1}$$

where the constant $A_1 = 0.170$ was determined recently by simulations.[30] The confinement free energy in the Odijk regime was studied analytically[40] and numerically[36,37] and is given by

$$F = A_2 N k_B T \left(\frac{a}{D}\right) \sqrt[3]{\frac{D}{l_P}} \tag{5.2}$$

with $A_2 = 2.46 \pm 0.07$. Using the same arguments as presented in the subsection on long chains with tail, one concludes that the force produced by the tail in the Odijk regime will be given by

$$\frac{f}{k_B T} = \frac{A_2}{D^2} \frac{\sqrt[3]{l_P/D}}{1 - A_1(2D/l_P)^{2/3}} \tag{5.3}$$

In a tube of the same diameter a stiff polymer with $l_P > 2D$ experiences a weaker tail-induced force than a flexible polymer with $l_P \ll D$. A crude estimate for not excessively small D/l_P ratios gives a relative decrease by a factor of 2 or 3 compared to flexible chain case.

Although we have omitted hydrodynamic interactions in our Monte Carlo simulations, they are certainly present and very important in nature. At the level of the scaling theory one can incorporate hydrodynamic interactions for tube geometry in a straightforward way.[26] At the level of a single blob the chain can be considered as nondraining with an effective friction coefficient per blob $\zeta_b \propto \eta D$ where η is the solvent viscosity. On the larger scale, hydrodynamic interactions are screened by the tube walls and the chain of blobs is effectively free-draining. Hence, the only change in the theoretical description of the ejection kinetics presented above would amount to a renormalization of the monomer friction coefficient. The free-draining monomer friction coefficient $\zeta \propto \eta D$ is to be replaced by ζ/g, where $g \propto (D/a)^{5/3}$ is the number of monomers per blob. This means that the renormalized monomer friction coefficient is smaller by a factor of $(a/D)^{2/3}$. Thus, in the presence of hydrodynamic interactions all the characteristic ejection times are reduced by a factor of $(a/D)^{2/3}$ as compared to the free-draining kinetics, but the shape of the $\tau(N)$ curves remains the same.

VI. Conclusion

The present paper provides a theoretical description of the ejection dynamics of a polymer chain out of confinement in terms of chain length N, pore length L, and its diameter D. We demonstrate that there exist two regimes of chain release for fully and partially confined macromolecules, depending on whether their length N is less or greater than a critical length $N^* \propto LD^{2/3}$. Thus, short chains that are fully confined in the pore leave the tube by diffusion. The mean ejection time τ depends then nonmonotonically on N. The largest residence time τ_{max} occurs for $N = N^*/3$.

The partially confined chains, in contrast, leave the pore after time $\tau = L^2D^{5/3}$ (regardless of N) due to a driving force exerted by the free tail on the confined part of the chain. This driving force is $\approx 5k_BT/D$ and is independent of the tail size. A rough estimate for the magnitude of this force yields $f \approx 15$ pN for a pore of diameter $D \approx 1.4$ nm (e.g., α-hemolysin) and $f = 2$ pN for $D \approx 10$ nm (*T*4-phage tail tube). Moreover, the magnitude of the force is universal for all polymers in tubes with $D \gg l_P$. Such a driving force pulls the chain out of the pore according to a time-reversed "capillary" law. The ratio τ_{max}/τ_{long} depends solely on the pore aspect ratio L/D.

The described mechanism applies to all flexible or semiflexible linear chains and may play an important role in translocation of polymers in biological systems. The distinct regimes of chain release from confinement could be utilized as a method for separation of DNA molecules as was demonstrated by Cabodi et al.[14] The theory of ejection times and times distributions presented in this paper could be then used as a basis of this potential method.

Acknowledgment. A.M. acknowledges support from the Deutsche Forschungsgemeinschaft (DFG) under Project No. Bi314/22. L.K. and A.S. are grateful to the DFG for financial support under Grant No. 436 RUS 113/863/0. A.S. also received partial support under RFBR No. 08-03-00402-a and 09-03-91344 NNIO-a.

References and Notes

(1) Alberts, B. In *Molecular Biology of the Cell*; Garland Publishing: New York, 1994.
(2) Kassianowicz, J. J.; Brandin, E.; Branton, D.; Deamer, D. *Proc. Natl. Acad. Sci. U.S.A.* **1996**, *93*, 13770.
(3) Meller, A.; Nivon, L.; Brandin, E.; Golovchenko, J.; Branton, D. *Proc. Natl. Acad. Sci. U.S.A.* **2000**, *97*, 1097.
(4) Teraoka, I.; Wang, Y. *Polymer* **2004**, *45*, 3835.
(5) Krasilnikov, O. V.; Rodrigues, C. G.; Bezrukov, S. M. *Phys. Rev. Lett.* **2006**, *97*, 018301.
(6) de Gennes, P. G. *Proc. Natl. Acad. Sci. U.S.A.* **1999**, *96*, 7262.
(7) Smith, D. E.; Tans, S. J.; Smith, S. B.; Grimes, S.; Andersen, D. L.; Bustamante, C. *Nature* **2001**, *413*, 748.
(8) Cacciuto, A.; Luijten, E. *Phys. Rev. Lett.* **2006**, *96*, 238104.
(9) Arsuaga, J.; Vazquez, M.; McGuish, P.; Trigueros, S.; Summer, D.; Roca, W. *Proc. Natl. Acad. Sci. U.S.A.* **2005**, *102*, 9165.

(10) Guevorkian, K.; Brochard-Wyart, F.; de Gennes, P.-G. In *Impact on Science*; Bok, J., Prost, J., Brochard-Wyart, F., Eds.; World Scientific: Singapore, 2009; Vol. *II*, p 69.
(11) Prinsen, P.; Fang, L. T.; Yoffe, A. M.; Knobler, C. M.; Gelbart, W. M. *J. Phys. Chem. B* **2009**, *113*, 3873.
(12) Turner, S. W. P.; Cabodi, M.; Craighead, H. G. *Phys. Rev. Lett.* **2002**, *88*, 128103.
(13) Reiner, W.; Morton, K. J.; Rühn, R.; Wang, Y. M.; Yue, Z.; Rosen, M.; Sturm, J. C.; Chou, S. Y.; Frey, E.; Aistin, R. H. *Phys. Rev. Lett.* **2005**, *94*, 196101.
(14) Cabodi, M.; Turner, S. W. P.; Craighead, H. G. *Anal. Chem.* **2002**, *74*, 5169.
(15) Daoud, M.; de Gennes, P. G. *J. Phys.* (*Paris*) **1977**, *38*, 85.
(16) Brochard-Wyart, F.; de Gennes, P. G. *J. Chem. Phys.* **1977**, *67*, 52.
(17) Kremer, K.; Binder, K. *J. Chem. Phys.* **1984**, *81*, 6381.
(18) Raphael, E.; Pincus, P. *J. Phys. II* **1992**, *2*, 1341.
(19) Milchev, A.; Binder, K. *Macromol. Theory Simul.* **1993**, *3*, 305.
(20) Sotta, P.; Lesne, A.; Victor, J. M. *J. Chem. Phys.* **2000**, *112*, 1565.
(21) Cifra, P. *J. Chem. Phys.* **2009**, *131*, 224903.
(22) Gong, Y.; Wang, Y. *Macromolecules* **2002**, *35*, 7492.
(23) Klushin, L. I.; Skvortsov, A. M.; Hsu, H. P.; Binder, K. *Macromolecules* **2008**, *41*, 5890.
(24) Hermsen, G. F.; M. Wesseling, G. F.; van der Veph, N. F. A. *Polymer* **2004**, *45*, 3027.
(25) Yang, Y.; Burkhard, T. M.; Gompper, G. *Phys. Rev. E* **2007**, *76*, 011804.
(26) de Gennes, P. G. *Scaling Concepts of Polymer Physics*; Cornell University Press: Ithaca, NY, 1979.
(27) Merlitz, H.; He, G.-L.; Sommer, J. U.; Wu, C. X. *Macromol. Theory Simul.* **2008**, *17*, 171.
(28) Salieb-Belugelaar, G. B.; Dorfman, K. D.; van den Berg, A.; Eijkel, J. C. T. *Lab Chip* **2009**, *9*, 2508.
(29) Milchev, A.; Binder, K. *Macromolecules* **1996**, *29*, 343.
(30) Cifra, P.; Benkova, Z.; Bleha, T. *Faraday Discuss.* **2008**, *139*, 377.
(31) Tegenfeldt, J. O.; Prinz, C.; Cao, H.; Chou, S.; Renner, W. W.; Rieches, R.; Wang, Y. M.; Cox, E. C.; Sturm, J. C.; Sillerzan, P.; Austin, R. H. *Proc. Natl. Acad. Sci. U.S.A.* **2004**, *101*, 10979.
(32) Burkhardt, T. W.; Guim, I. *Phys. Rev. E* **1999**, *59*, 5833.
(33) Hsu, H. P.; Binder, K.; Klushin, L. I.; Skvortsov, A. M. *Phys. Rev. E* **2007**, *76*, 021108.
(34) Hsu, H. P.; Binder, K.; Klushin, L. I.; Skvortsov, A. M. *Phys. Rev. E* **2008**, *78*, 041803.
(35) Odijk, T. *Phys. Rev. E* **2008**, *77*, 060901.
(36) Dijkstra, M.; Frenkel, D.; Lekkerkerker, H. N. W. *Physica A* **1993**, *193*, 374.
(37) Bicout, D. J.; Burkhardt, T. W. *J. Phys. A: Math. Gen.* **2001**, *34*, 5745.
(38) Redner, S. *A Guide to First-Passage Processes*; Cambridge University Press: New York, 2001.
(39) Risken, H. *The Fokker Planck Equation: Methods of Solutions and Applications*; Springer: Berlin, 1989.
(40) Burkhardt, T. *J. Phys. A: Math. Gen.* **1977**, *30*, L167.